


Exploiting antidiabetic activity of silver nanoparticles synthesized using Punica granatum leaves and anticancer potential against human liver cancer cells (HepG2)

Rijuta G. Saratale, Han Seung Shin, Gopalakrishnan Kumar, Giovanni Benelli, Dong-Su Kim & Ganesh D. Saratale



To cite this article: Rijuta G. Saratale, Han Seung Shin, Gopalakrishnan Kumar, Giovanni Benelli, Dong-Su Kim & Ganesh D. Saratale (2017): Exploiting antidiabetic activity of silver nanoparticles synthesized using Punica granatum leaves and anticancer potential against human liver cancer cells (HepG2), *Artificial Cells, Nanomedicine, and Biotechnology*, DOI: [10.1080/21691401.2017.1337031](https://doi.org/10.1080/21691401.2017.1337031)

To link to this article: <http://dx.doi.org/10.1080/21691401.2017.1337031>

 View supplementary material 

 Published online: 14 Jun 2017.

 Submit your article to this journal 

 View related articles 

 View Crossmark data 



Exploiting antidiabetic activity of silver nanoparticles synthesized using *Punica granatum* leaves and anticancer potential against human liver cancer cells (HepG2)

Rijuta G. Saratale^a, Han Seung Shin^b, Gopalakrishnan Kumar^{c*}, Giovanni Benelli^d, Dong-Su Kim^e and Ganesh D. Saratale^b

^aResearch Institute of Biotechnology and Medical Converged Science, Dongguk University-Seoul, Goyang-si, Republic of Korea; ^bDepartment of Food Science and Biotechnology, Dongguk University-Seoul, Goyang-si, Republic of Korea; ^cDepartment of Environmental Engineering, Daegu University, South Korea; ^dDepartment of Agriculture, Food and Environment, University of Pisa, Pisa, Italy; ^eDepartment of Environmental Science and Engineering, Ewha Womans University, Seoul, South Korea

ABSTRACT

This study first time reports the novel synthesis of silver nanoparticles (AgNPs) using a *Punica granatum* leaf extract (PGE). The synthesized AgNPs were characterized by various analytical techniques including UV-Vis, Fourier transform infrared (FTIR), X-ray powder diffraction (XRD), X-ray photoelectron spectroscopy (XPS), field emission scanning electron microscopy and energy-dispersive spectra (FESEM-EDS) and high-resolution transmission electron microscopy (HRTEM). FTIR analysis revealed that the involvement of biological macromolecules of *P. granatum* leaf extract were distributed and involved in the synthesis and stabilization of AgNPs. A surface-sensitive technique of XPS was used to analyse the composition and oxidation state of synthesized AgNPs. The analytical results confirmed that the AgNPs were crystalline in nature with spherical shape. The zeta potential study revealed that the surface charge of synthesized AgNPs was highly negative (-26.6 mV) and particle size distribution was ranging from ~ 35 to 60 nm and the average particle size was about 48 nm determined by dynamic light scattering (DLS). The PGE-AgNPs antidiabetic potential exhibited effective inhibition against α -amylase and α -glucosidase (IC_{50} : 65.2 and 53.8 $\mu\text{g/mL}$, respectively). The PGE-AgNPs showed a dose-dependent response against human liver cancer cells (HepG2) (IC_{50} : 70 $\mu\text{g/mL}$) indicating its greater efficacy in killing cancer cells. They also possessed *in vitro* free radical-scavenging activity in terms of ABTS (IC_{50} : 52.2 $\mu\text{g/mL}$) and DPPH (IC_{50} : 67.1 $\mu\text{g/mL}$) antioxidant activity. PGE-AgNPs displayed strong antibacterial activity and potent synergy with standard antibiotics against pathogenic bacteria. Thus, synthesized PGE-AgNPs show potential biomedical and industrial applications.

ARTICLE HISTORY

Received 20 May 2017
Accepted 22 May 2017

KEYWORDS



α -Glucosidase; anticancer activity; liver cancer HepG2 cell line; *in vitro* antioxidant activity; *Punica granatum* leaf extract

Introduction


In recent years, nanotechnology has become a leading research field in health and medicine. Nanomedicine has made a rapid and broad impact on health care and provided a plethora of possibilities in various industries and scientific endeavours [1]. Nanoparticles (NPs) are more biocompatible than conventional therapeutics. Thus, NPs can be exploited for drug encapsulation and site-specific delivery, increasing the drug efficacy compared to larger-sized particles and assisting to reduce the undesired toxicity of the drug [1,2]. A literature survey suggests that NPs have enhanced antimicrobial activity because they can evade the immune response by crossing through impermeable membranes [3]. Silver nanoparticles (AgNPs) are gaining predominant interest due to their remarkable properties, such as good conductivity, chemical stability, antibacterial and antifungal activity, and anticancer, antidiabetic and antiinflammatory potential [2,4].

A metabolic disorder known as "diabetes" is usually considered as elevated glucose level in the blood presently affecting more than 100 million people worldwide [5]. Thus, there is an urgent need to develop nanomedicine which can facilitate significant inhibition of carbohydrate-hydrolysing enzymes with high degree of specificity as well as to achieve maximal therapeutic efficacy with minimal side effects [6]. Cancer is a group of diseases which causes abnormal cell growth and having ability to spread and thus remains one of the world's most devastating disease. There are various treatment options including surgery, radiation and chemotherapeutic drugs but during this treatment mostly kill healthy cells and produces toxicity. The rapidly developing field of various nanomaterials and nanodevices using AgNPs has increased the possibility for the early diagnosis and treatment of cancer with least adverse effects [7-11].

Antioxidants play a major role in balancing the free radicals since these free radicals mostly attack macromolecules

CONTACT Ganesh D. Saratale  gdsaratale@dongguk.edu  Department of Food Science & Biotechnology, Dongguk University-Seoul, 32 Dongguk-ro, Ilsandong-gu, Goyang-si, Gyeonggi-do, 10326, Korea

*Green Processing, Bioremediation and Alternative Energies Research Group (GPBAE), Faculty of Environment and Labour Safety, Ton Duc Thang University, Ho Chi Minh City, Vietnam

 Supplemental data for this article can be accessed here.

© 2017 Informa UK Limited, trading as Taylor & Francis Group

(lipids, proteins and nucleic acids) which lead to cell damage. The higher accumulation of reactive species leads to diverse chronic pathologies, such as development of cancer, cardiovascular and neurodegenerative diseases [12–15]. The literature suggests that AgNPs display considerable antioxidant activity *in vitro*; however, their clinical significance has not yet been determined well [16–17]. In the past two decades, human pathogens mainly bacteria have developed resistance against most of the antibiotics resulting their decreasing efficacy. This problem is a challenge in medical science, and there is an urgent need to find environmentally benign bio-material/bioresources in the synthesis of silver nanoparticles and their synergistic role with antibiotics to improve antimicrobial properties with the prospect of untreatable infections [8].

The use of plant extracts for the synthesis of AgNPs are most promising due to their viability, low cost and eco-friendliness that brings significant opportunity to synergize green chemistry and nanosynthesis [18]. Biomacromolecules/phytochemicals from plant extracts have continued to receive unprecedented attention, because they are believed to have antibiotic, anthelmintic, and antitumor properties. It also reduces the use of toxic and hazardous substances and serves as potential capping and stabilization molecules of NPs [19–20]. The use of plant leaves to synthesize AgNPs is popular because it offers a facile and affordable process compared to synthetic techniques and can yield well-characterized NPs [21]. A literature survey proves that leaf extracts from various plants, such as *Argyrea nervosa* [22], *Terminalia cuneata* [23], *Tamarix gallica* [24], *Mussaenda erythrophylla* [19], *Prunus yedoensis* [25], *Iresine herbstii* [14], *Clerodendrum phlomidis* [26], *Lonicera japonica* [16], *Abutilon indicum* [15], *Lantana camara* [13], *Rosmarinus officinalis* [20], *Catharanthus roseus* [27] and *Prunus japonica* [28] can be used to synthesize AgNPs.

Pomegranate, *Punica granatum* (L.) is an ancient fruit belonging to the Punicaceae family. It is found in more arid regions of Southeast Asia, the East Indies and tropical Africa [29]. Pomegranate juice is a rich source of flavonoids, alkaloids and ellagic acid and has been used as a remedy for diabetes in the Unani system of medicine practiced in the Middle East and India [30]. The leaves of *P. granatum* are glossy and lance-shaped and their extracts contain ellagic acid, tannins (punicalin and punicafolin) and flavone glycosides (luteolin and apigenin) [31].

The current study aimed to develop a cost-effective green synthesis of AgNPs using a *P. granatum* leaf extract (PGE). The synthesized AgNPs were characterized using several microscopic and spectroscopic techniques. The *in vitro* free radical-scavenging potency and antidiabetic potential of the AgNPs was also evaluated. Furthermore, we investigated the anticancer activity of the AgNPs against a liver cancer cell line (HepG2) based on their ability to inhibit cell viability. The synergistic antibacterial activity of AgNPs with standard antibiotics was determined. Until now very few reports show the use of *P. granatum* peel extract for the synthesis of gold nanoparticles and there is no detail study on the use of *P. granatum* leaves for AgNPs reported. In this study, we first

time report *P. granatum* leaves mediated synthesis of silver NPs and to evaluate their various biological properties.

Materials and methods

Chemicals and microorganisms used

Silver nitrate (AgNO_3 , 99%) was obtained from Sigma–Aldrich (St. Louis, MO). All other chemicals required for antibacterial, antioxidant, antidiabetic and anticancer studies were of the highest purity available and of analytical grade. All glassware was washed with non-ionic detergent, rinsed with Millipore–Milli-Q distilled water and ethanol multiple times to remove the detergent and then dried before use. *Staphylococcus aureus* and *Escherichia coli* cultures were used model microorganisms for antibacterial studies. Commercial antibiotic discs containing vancomycin, streptomycin, oxytetracycline, gentamicin and amoxicillin, were, respectively, purchased from Liofilchem, Italy.

Preparation of the PGE

Fresh *P. granatum* leaves were collected and washed with tap water, and then, surface washed with Milli-Q water until no impurities remained. The dirt-free leaves were dried in the shade at room temperature for 10 days to remove residue moisture. The dried leaves were pulverized in a sterile electric blender to obtain a fine powder and stored in an airtight bottle, avoiding sunlight. An aliquot of the leaf powder (5 g) was mixed thoroughly with 100 mL of Milli-Q water and then boiled at 60 °C for 15 min, followed by cooling and filtration through Whatman no. 1 filter paper to obtain the leaf extract. The filtered extract was collected and used for AgNPs synthesis.

Synthesis of AgNPs

PGE was mixed with an aqueous solution of AgNO_3 (1 mM) (1:10 mixing ratio) at pH 5.0, at room temperature. The colour change (pale yellow to dark reddish-brown), indicating the chemical reduction, and thus, the AgNPs formation was monitored by UV-vis spectrometry at 300–600 nm and occurred within 20 min. The stability of the synthesized AgNPs was monitored at room temperature for up to 6 months. A change in surface plasmon resonance (SPR) of the AgNPs was detected through UV-vis measurements. The synthesized AgNPs were separated by centrifugation at 12,000 rpm for 20 min (Labogene, 1736 R). The obtained pellets were re-dispersed in sterile deionized water three times to remove any free biomass residue. The purified pellets were oven-dried at 60 °C for 12 h and the dried AgNPs were scrapped out for further characterization.

Characterization of AgNPs

The aqueous extract was monitored by using a UV-vis spectrophotometer (Optizen, Model 2120 UV plus) over 300–600 nm at regular time intervals to determine the time

point of maximum production of the AgNPs. X-ray powder diffraction (XRD) patterns of the AgNPs were recorded with 2θ scans from 30 to 80° at 0.04° per min with a time constant of 2 s by an X-ray diffractometer (Rigaku, Japan). The same sample thin film without scratch was used for X-ray photoelectron spectroscopy (XPS) analysis to measure the elemental composition using (Veresprobe II, Japan).

Fourier transform infrared (FTIR) (Perkin Elmer, Norwalk, CT) spectra of PGE and PGE-synthesized AgNPs were acquired to reveal the combination and distribution of biological macromolecules on the surface of the NPs. Spectra over the 4000–400 cm^{-1} range were obtained by the coaddition of 32 scans at a resolution of 4 cm^{-1} .

The surface morphology and elemental composition of the NPs were studied by using field emission scanning electron microscopy (FESEM) and energy-dispersive spectra (EDS) (JEOL-64000, Japan). The acceleration voltage and the emission current were 15 kV and 12 μA , respectively, from a cold field emission gun. Small amounts of sample were dropped on a carbon-coated copper grid then gold-coated to prepare thin films. The films were dried with a mercury lamp for 5 min. The surface morphology and size distribution of the NPs were observed with high-resolution transmission electron microscopy (HRTEM) images and selective area diffraction patterns (SAED) were recorded using a Tecnai G2 20S-TWIN (FEI Company) instrument. The related size distribution pattern of the AgNPs was plotted by manual counting of 100 individual particles from various TEM images.

The particle size distribution and zeta potential analysis of biosynthesized AgNPs were evaluated. Zeta potential analysis was done by using ELS-8000 (OTSUKA Ltd., Japan). DLS is particularly employed for sizing nanoparticles and determining their state of aggregation in suspensions. Dynamic light scattering (DLS) analysis was performed on BI-9000AT (Brookhaven, NY) in the range of 0.1–1000 μm at 25 °C.

Determination of biological potential of PGE-AgNPs

Antidiabetic potential of biosynthesized AgNPs

The α -amylase assay mixture, consisting of sodium phosphate buffer (0.5 mL, 0.02 M, pH 6.9) containing α -amylase (1 U/mL) and AgNPs 20–100 $\mu\text{g}/\text{mL}$, was pre-incubated at 37 °C for 20 min. A 250 μL aliquot of starch solution (1%) was added to the tubes, which were further incubated at 37 °C for 15 min. The reaction was then terminated by adding 1 mL of dinitrosalicylic acid reagent and heating in a boiling water bath for 10 min [32]. The tubes were further cooled and the absorbance was recorded at 540 nm. The α -glucosidase inhibition was determined according to a modified method [16]. The assay mixture, consisting of 150 μL of 0.1 M sodium phosphate buffer (pH 6.9), α -glucosidase (1 U/mL), and AgNPs at 20–100 $\mu\text{g}/\text{mL}$, was preincubated at 37 °C for 10 min. Then, 50 μL of 2 mM para-nitrophenyl- α -D-glucopyranoside in sodium phosphate buffer was added to the mixture and incubated at 37 °C for 20 min. The reaction was terminated by adding 50 μL of 0.1 M sodium carbonate (Na_2CO_3). The absorbance was measured at 405 nm. In both enzyme assays, the tube with enzyme but without AgNPs served as the

control with 100% enzyme activity. Acarbose served as the positive control. The inhibitory activity was expressed as the percentage of inhibition.

Anticancer activity of AgNPs against the HepG2 cell line

The anticancer activity of the PGE and AgNPs and the cytotoxicity potential of the PGE-AgNPs was determined by the MTT (3-(4,5-dimethyl thiazol-2yl)-2,5-diphenyl tetrazolium bromide) assay using HepG2 cells. Human liver cancer cell line (HepG2) was obtained from American Tissue Culture Collection (ATCC). The cells were cultured and maintained in RPMI 1640 media supplemented with 10% foetal bovine serum). The cells were maintained in monolayer culture at 37 °C under a humidified atmosphere of 5% CO_2 . The cells were subcultured by trypsinization (0.025% trypsin and 0.0025% EDTA) and maintained in tissue culture laboratory. The cells were grown in 96-well microtitre plates at 1.25×10^4 cells/well for 24 h. For the MTT assay, the medium from the wells was carefully removed after incubation. The cells were washed twice with 100 μL of serum-free medium and starved for an hour at 37 °C in a CO_2 incubator. Then, the cells were treated with PGE and various concentrations of AgNPs (5–100 $\mu\text{g}/\text{mL}$) and incubated for 24 h. A 20 μL aliquot of MTT reagent (10%) was then added to each well and the plates incubated in a water bath at 37 °C for 4 h. Then, DMSO (10%) was added and the plates agitated for 30 min using a plate shaker in the dark. Finally, the absorbance of the samples (including the blanks) was measured in a microtitre plate reader at 590 nm (Biotek, Epoch microplate spectrophotometer, Winooski, VT). The results were expressed as the IC_{50} values (effective concentration showing 50% inhibition of activity) of the respective MTT assay. The percentage of cell viability was calculated to obtain the anticancer potential of the AgNPs.

In vitro free radical scavenging activity of biosynthesized AgNPs

The DPPH scavenging effect of the AgNPs solution was determined according to an earlier study [16]. About 2 mL of DPPH (2,2-diphenyl-1-picrylhydrazyl) solution was added to 0.2 mL of various concentrations of the AgNPs solution. The mixture was vortexed and kept at room temperature for 30 min in the dark to allow DPPH radical scavenging to occur. The absorbance of the solution was then measured at 517 nm using catechol solution as a standard. For the ABTS assay, ABTS salt (7.0 μM) and potassium persulphate (2.45 μM) were combined to produce the ABTS^+ and kept in the dark at 25 °C for 16 h. A portion of the ABTS^+ solution was diluted with 80% (v/v) ethanol to an absorbance between 0.700 ± 0.005 at 734 nm using a spectrophotometer [33]. An aliquot (0.2 mL) of the AgNPs solution at various concentrations was combined with 2 mL of ABTS^+ solution and the reaction mixture vortexed for 10 s immediately and after 6 min. Then, the absorbance was read spectrophotometrically at 734 nm using ascorbic acid as a standard. A blank experiment (without NPs) was also carried out. All assays were performed in triplicate. The results were expressed as the IC_{50} values (effective concentration showing

50% inhibition of activity). The scavenging percentages of DPPH and ABTS⁺ radicals by the NPs were calculated using the formula reported earlier [11,22]:

$$\text{Free radical scavenging (\%)} = \frac{[AC - AT]}{AC} \times 100$$

where AC is the absorbance of the DPPH and ABTS⁺ controls in the respective assays, while AT is the absorbance of DPPH and ABTS⁺ free radicals in the presence of NPs, at 517 and 734 nm, respectively.

Synergistic antibacterial potential of AgNPs with standard antibiotics

Initially, the antimicrobial activity of the PGE and synthesized AgNPs were tested against Gram-positive and Gram-negative bacteria including *Staphylococcus aureus* and *Escherichia coli* by the standard agar disc diffusion method [34]. Each individual culture (100 μL) was uniformly spread onto the Luria–Bertani agar plates using glass rods. Then, 25 μL of PGE (control) and 25 μL of AgNPs were loaded on each sterile Whatman no. 1 paper disc (5 mm diameter) placed on each plate. The combined *in vitro* antibacterial activity of the AgNPs and antibiotics, vancomycin, streptomycin, oxytetracycline, gentamicin and amoxicillin against *E. coli* and *S. aureus* were also evaluated by further impregnating the discs with 25 μL of the synthesized AgNPs. Standard sterile antibiotic discs were used as the positive control. The plates were incubated at 37 °C for 24 h and the bactericidal activity evaluated by the size of the clear zone. The greater the zone of inhibition, the greater is the bactericidal activity. The synergistic antibacterial activity was documented by calculating the increase in fold area of the zone of inhibition using the following formula:

$$\text{Fold area in zone of inhibition (\%)} = \frac{[B - A]}{A} \times 100$$

where “A” and “B” refer to the zones of inhibition for antibiotic alone and AgNPs impregnated with antibiotics, respectively.

Statistical analysis

Anticancer, antimicrobial and radical scavenging data were analysed using analysis of variance (ANOVA) followed by Tukey’s HSD test ($p < .05$). JMP 11 was used for all the analyses.

Results and discussion

UV–Vis spectra study of synthesized AgNPs

As a fundamental analytical technique, UV-vis spectroscopy was done to confirm the formation of AgNPs. Indeed, when PGE was added to the AgNO₃ solution, it transformed from a pale-yellow solution to a dark brown at room temperature within 20 min. The spectra of the AgNPs showed a maximum SPR peak at about 415 nm, which is the characteristic absorbance band for AgNPs (Figure 1), which is observed in literature studies at 410–450 nm [13,19]. The presence of

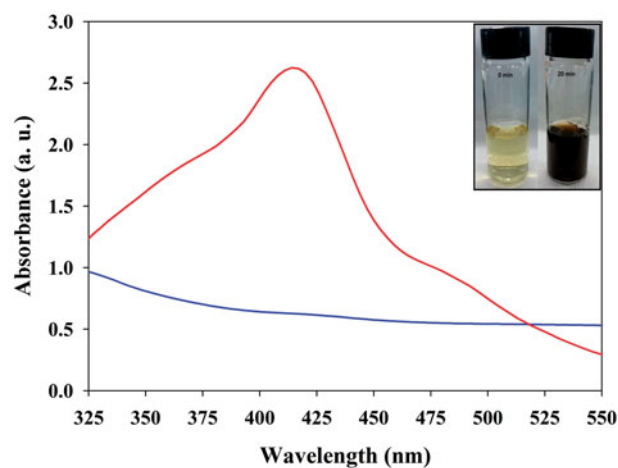


Figure 1. UV–Vis spectral analysis of *Punica granatum* leaf extract (PGE) and synthesized PGE-AgNPs after incubation at room temperature for 20 min (inset is the digital photographs of the corresponding AgNPs).

phytochemicals, such as phenolics, flavonoids, tannins and alkaloids, present in the leaf extract play a key role in the conversion of the ionic form of silver to the metallic nanoform [30–31]. The possible mechanism of AgNPs formation, capping and stabilization using PGE is illustrated in Figure 2.

XRD analysis of synthesized AgNPs

The XRD pattern of the synthesized AgNPs is shown in Figure 3. The diffraction peaks at $2\theta = 38.1, 44.2^\circ, 64.4^\circ$ and 77.4° were assigned to the corresponding diffraction signals (111), (200), (220) and (311), respectively, which indicate the face-centred cubic crystalline AgNPs (Joint Committee on Powder Diffraction Standards; JCPDS no. 04-0783). The high intensity of reflection (111) relative to the other reflections (Figure 3), indicates the silver nanocrystals because these peaks are mainly oriented along the (111) plane [35]. The results are consistent with previous studies, reporting similar diffraction peaks of AgNPs [25,35].

XPS analysis of synthesized AgNPs

XPS study provides the surface chemical nature and oxidation state of the synthesized AgNPs. Figure 4(A) is the XPS survey spectrum for the product showing the presence of Ag, O, OKLL, AgMNN elements at their respective binding energy positions due to the binding of PGE biochemical constituents with AgNPs. The strong sharp signal of Ag3d at 370 eV shows the presence of Ag metal. High resolution XPS spectrum of the Ag3d was evaluated to check the valence state of AgNPs in the assembly (Figure 4(B)). The binding energies of Ag3d3 and Ag3d5 were identified at 373.85 eV and 367.60 eV, respectively and the splitting of the 3d doublet of Ag was ~6 eV, indicates the existence of AgNPs at their Ag⁰ state [13].

FTIR analysis of PGE and PGE-synthesized AgNPs

FTIR spectra revealed the combination and distribution of biological macromolecules of PGE on the surface of the AgNPs.

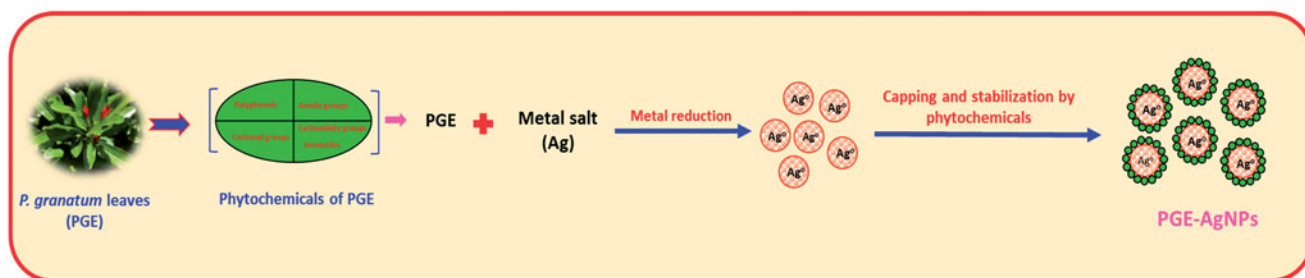


Figure 2. Schematic representation of the synthesis, capping and stabilization of AgNPs using *Punica granatum* leaf extract.

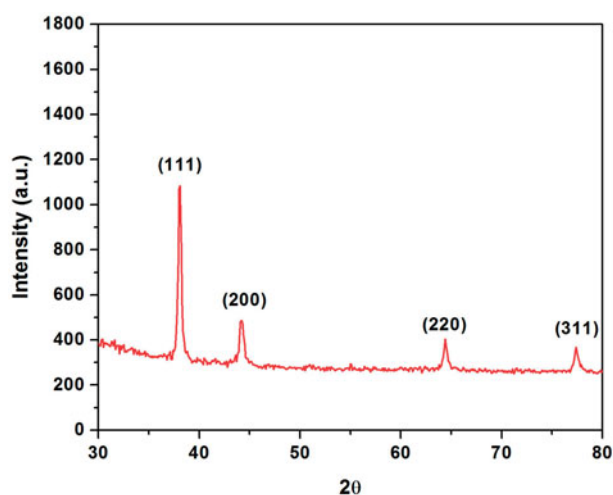


Figure 3. XRD pattern of the synthesized PGE-AgNPs.

FTIR analysis was performed to determine the functional groups involved in the reduction of silver into the respective AgNPs by the PGE. The FTIR spectra of the aqueous leaf extract of *P. granatum* and the synthesized AgNPs, shown in Figure 5, respectively, revealed strong absorption peaks at 3400 and 3384 cm^{-1} , 2940 and 2928 cm^{-1} , 1640 and 1632 cm^{-1} , 1438 and 1428 cm^{-1} and 1070 and 1058 cm^{-1} , respectively. The peak IR bands observed at 3400 and 3384 cm^{-1} are characteristic of the O–H and C=O groups, possibly due to polyphenols, such as flavonoids or aromatic acids, present in the leaf extract [13,17]. The peaks at 2940 and 2933 cm^{-1} are assigned to the asymmetric and symmetric C–H stretching (alkanes) vibration of flavonoids, respectively [36]. The peaks at 1640 and 1632 cm^{-1} derive from the –C–C– stretching vibration in the aromatic ring [37]. The absorption peaks at 1438 and 1428 cm^{-1} represent –C–C stretching mode, confirming the presence of an aromatic group [36–37]. The peaks at 1070 and 1058 cm^{-1} are assigned to C–OH stretching of secondary alcohols [38]. The relative shift of these peak positions and intensity distribution in the IR of the two spectra (Figure 5) indicates that different functional groups of the PGE were probably involved in the AgNPs formation, and play an important role in the capping and stabilization, which helps avoid the AgNPs agglomeration.

Morphological and elemental analysis of synthesized AgNPs by FESEM and EDS

The morphology and size analysis of the synthesized AgNPs, which were investigated by FESEM, showed that the particles

were spherical in shape and small in size (Figure 6(A)). A slight agglomeration of the synthesized AgNPs was noticed. However, each agglomerate was composed of small crystallites. The EDS spectrum of the PGE synthesized AgNPs shows the intense silver peak at 3 keV (Figure 6(B)), which is the characteristic absorption of metallic silver due to SPR [22,35] and provides the qualitative and quantitative status of elements. The presence of small peaks corresponding to Cl, C, O and S in the EDS spectrum confirmed the existence of the biomolecules of PGE on the surface of the synthesized AgNPs. The quantitative analysis gives the weight percentage of all the elements present in the synthesized AgNPs (Figure 6(B)). The EDS results showed the highest proportion of silver was 89.9%, which is evidence of the green synthesis of AgNPs.

HRTEM analysis of synthesized AgNPs

HRTEM showed that most of the AgNPs were uniform spherical NPs with an average size of ~20–45 nm and some were variably distributed (Figure 7(A)). The SAED pattern, shown in Figure 7(B) has bright circular rings corresponding to the (111), (200), (220) and (311) planes, revealing the highly polycrystalline nature of the AgNPs, consistent with the XRD results and previous literature studies [39–40].

Stability studies of synthesized AgNPs

The stability of the synthesized PGE-AgNPs recorded over 6 months showed no aggregation or any significant change in the SPR. Thus, the synthesized AgNPs were stable and could, therefore, be useful for various biomedical applications (Figure 8(A)). In addition to this, we have analysed the DLS and zeta potential, in order to know the stability and charge of the synthesized PGE-AgNPs. Zeta potential is an important parameter that represents the surface charge of NPs, predicting interactions between NPs and useful to foretell the long-term stability of NPs in suspension [13]. The literature survey suggests that if the NPs with higher negative (–25 mV) or positive (+25 mV) zeta potential, then they will repel each other and showed high degrees of stability [41]. The zeta potential value of dispersed synthesized PGE-AgNPs in deionized water in the absence of any electrolyte was –26.6 mV (Figure 8(B)). The negative charge on PGE-AgNPs confirms the repulsion among the particles, and thus, particles do not undergo coalescence avoiding agglomeration, which supports the long-term stability of synthesized AgNPs. Moreover, the

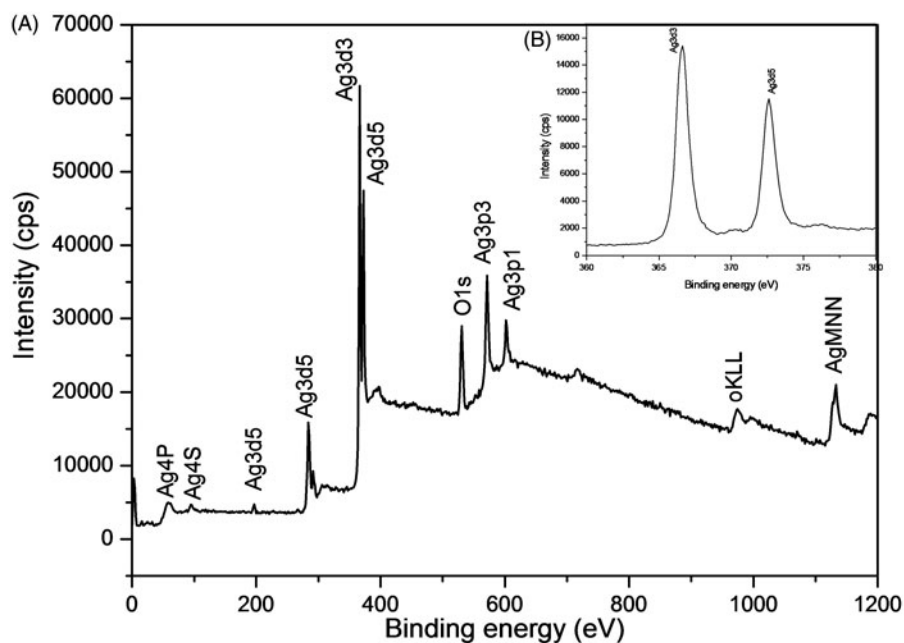


Figure 4. XPS spectra of (A) Survey and (B) Ag 3d of the synthesized PGE-AgNPs.

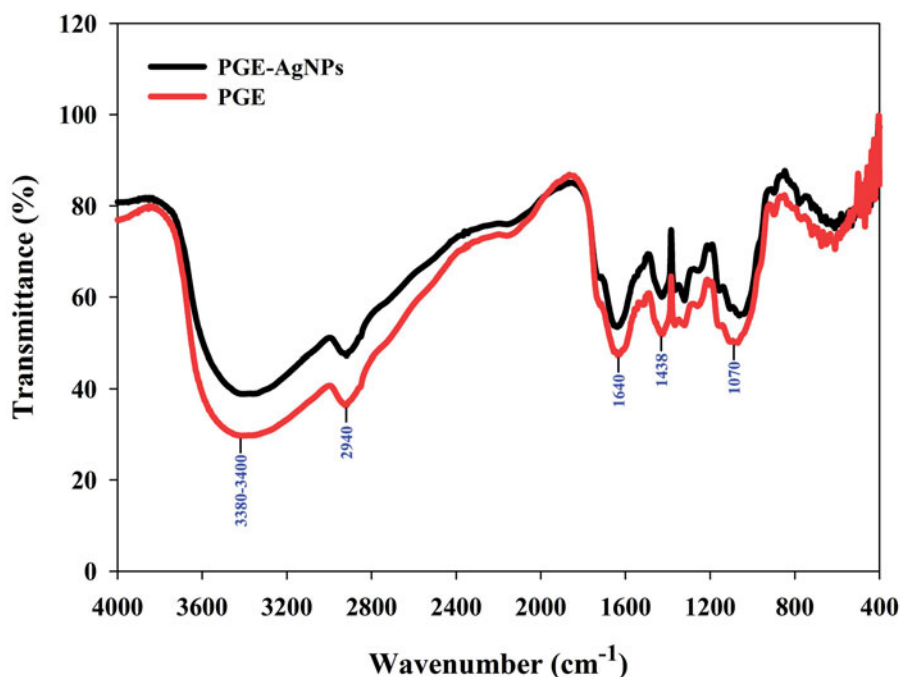


Figure 5. FTIR spectra of *Punica granatum* leaf extract (PGE) and synthesized PGE-AgNPs.

zeta potential of NPs strongly depends on pH and electrolyte concentration of the dispersion [13,41]. The DLS size distribution image of PGE-AgNPs is depicted in Figure 8(C). Particle size distribution curve reveals that AgNPs obtained are poly-dispersed in nature. It was observed that the size distribution of AgNPs ranges from ~35 to 60 nm. The calculated average particle size distribution of AgNPs is 48 nm (Figure 8(C)).

Antidiabetic potential of PGE-AgNPs

Diabetes mellitus is a group of metabolic diseases in which there are high blood sugar levels over a prolonged period.

A therapeutic approach to decrease the hyperglycaemia is to inhibit the carbohydrate digesting enzymes (α -glucosidase and α -amylase), thereby preventing the breakdown of carbohydrates into monosaccharides which is a main cause of increasing blood glucose level [6,42]. Therefore, developing compounds having inhibitory activities towards carbohydrate hydrolysing enzymes may be a useful way to manage diabetes [6,42]. As shown in Figure 9(A,B), α -amylase and α -glucosidase were significantly inhibited in a dose-dependent manner by the PGE-AgNPs. The results suggest that with the increased AgNPs concentration, the activity levels of enzyme were remarkably reduced, producing IC_{50} values of 65.2 and 53.8 μ g/mL, respectively, which

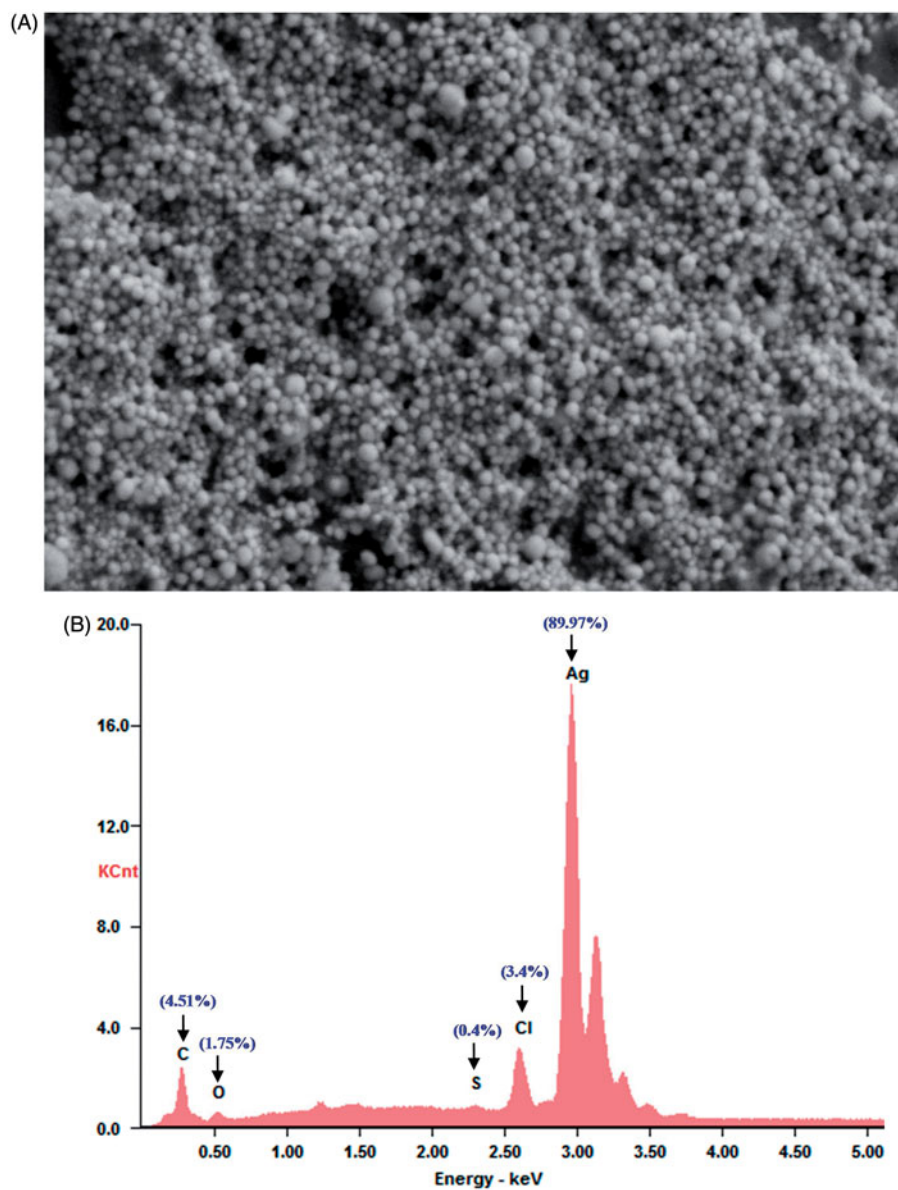


Figure 6. (A) FESEM images and (B) EDS spectrum of synthesized PGE-AgNPs.

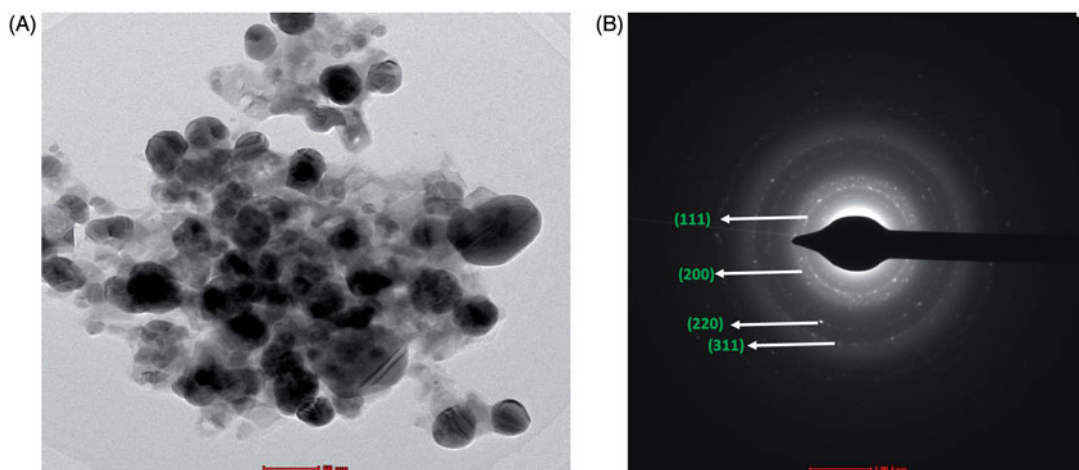


Figure 7. (A) HRTEM micrographs of PGE-AgNPs and (B) SAED results illustrating the formation of AgNPs.

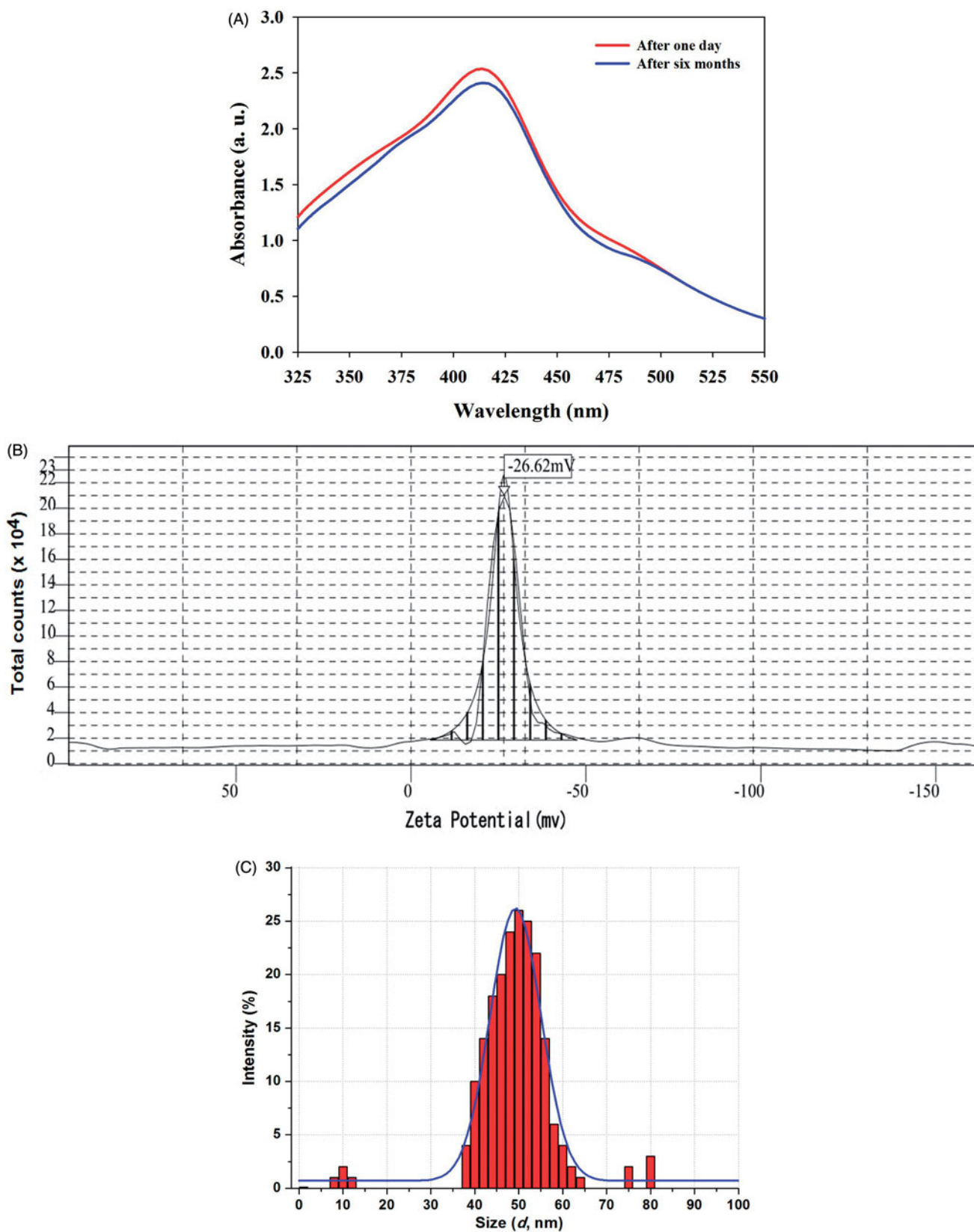


Figure 8. Stability of synthesized PGE-AgNPs up to 6 months and their (A) SPR spectrum, (B) zeta potential and (C) particle size distribution determined by DLS.

were significantly higher than the PGE (Figure 9(a,b)). Hence, the PGE biomolecules likely enhanced the antidiabetic potential of the synthesized NPs. α -Amylase and α -glucosidase inhibitory actions were observed in increasing

order, as PGE < AgNPs < Acarbose (Figure 9). Comparable results were observed in the literature [16,43]. However, the foregoing results suggest that the synthesized PGE-AgNPs are potentially better antidiabetic particles at

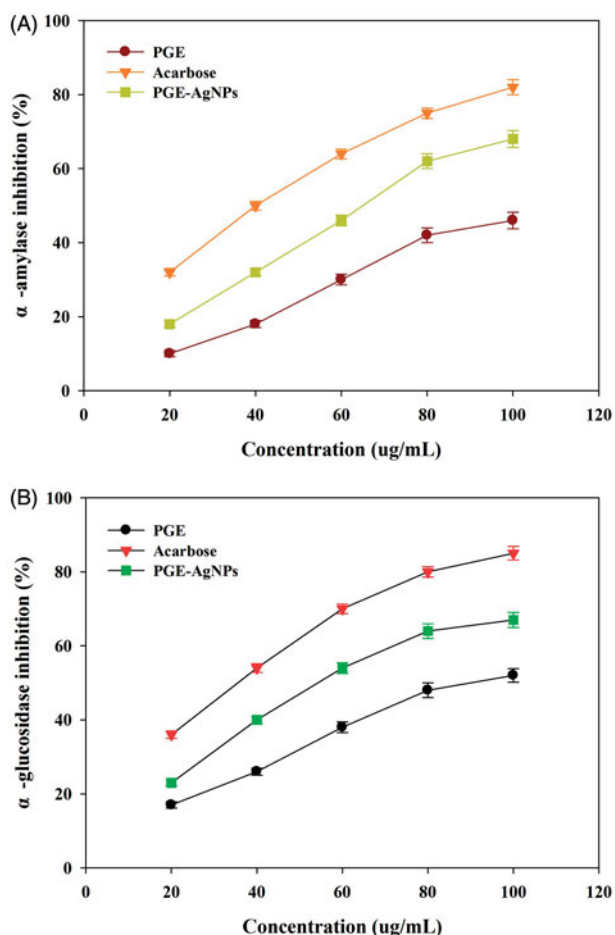


Figure 9. Antidiabetic activity of synthesized PGE-AgNPs based on inhibition of α -amylase and α -glucosidase activity.

inhibiting carbohydrate digesting enzymes, and could prove an effective approach in the diabetes care.

In vitro cytotoxicity assessment of biosynthesized AgNPs

In vitro cytotoxicity against the HepG2 cell line was studied by the MTT assay using various concentrations of PGE-AgNPs (5, 10, 20, 40, 60, 80, 100, 150 and 200 $\mu\text{g/mL}$). Figure 10 shows that the AgNPs possess significant anticancer activity and approximately 70 $\mu\text{g/mL}$ is required to induce 50% cell mortality. In contrast, 200 $\mu\text{g/mL}$ AgNPs significantly inhibited cell growth by more than 90% (Figure 10), whereas the PGE showed low cytotoxicity (about 10%) (Figure 10). The anticancer activity was directly dose-dependent, demonstrating the pivotal role of the AgNPs concentration. Our results collaborated earlier observations with AgNPs against MCF-7 breast cancer cells [44], rat glial tumor C6 cells [11], Dalton's lymphoma ascites [45], lung A-549 carcinoma cells [46], lung cancer cell lines (A549) and cervical cancer cell line (HeLa) [47], colon cancer cell lines (HT29) [48] and the HepG2 liver cancer cell line [43]. The inhibitory mechanism of AgNPs against cancer cell lines has not been well known. However, it was supposed that AgNPs can block the activity of abnormally multiplied signalling proteins or interact with functional groups of intracellular proteins and enzymes, as well as with the nitrogen bases in DNA, which results in cell death [45–49]. Nevertheless, this is the first report on the cytotoxic effects of PGE-synthesized AgNPs using the HepG2 liver cancer cell line. Further investigations are, therefore, required to identify the possible mechanism involved in the anticancer activity.

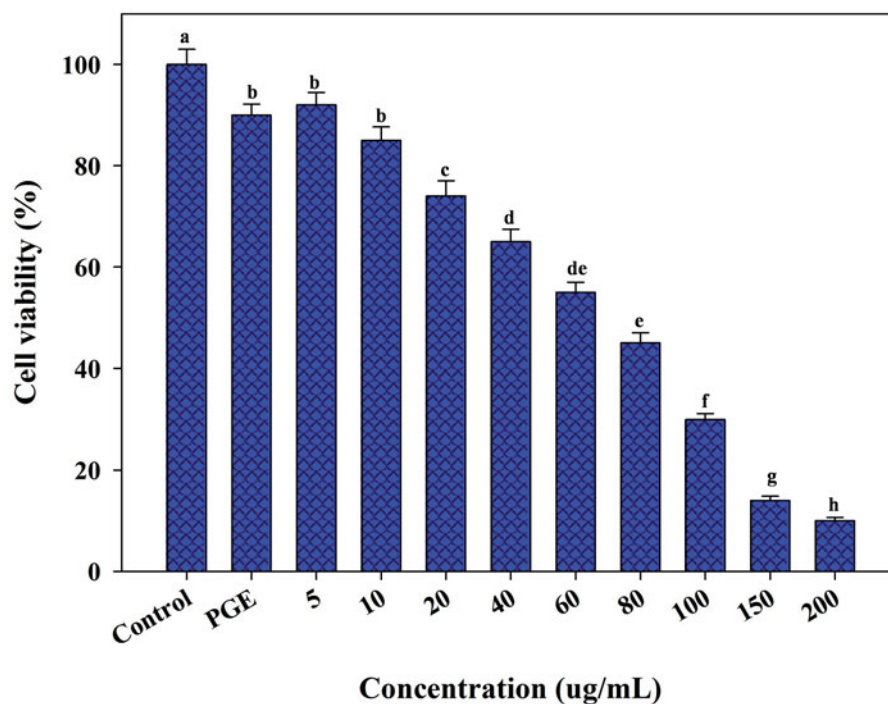


Figure 10. Anticancer activity of various concentrations of synthesized PGE-AgNPs against the liver cancer cell line- HepG2 (within each tested dose, different letters above each column indicate significant differences).

DPPH and ABTS radical-scavenging activity of PGE-AgNPs

The DPPH and ABTS⁺ free radical-scavenging antioxidant potential of the synthesized NPs (Figure 11(A,B)) indicated that their DPPH activity was dose dependent, with increased inhibition of 80%, 64% and 48% at 100 µg/mL for catechol, AgNPs and PGE, respectively. The AgNPs were found to be effective against the DPPH radicals, displaying an IC₅₀ value of 67 µg/mL (Figure 11(A)). This result concurs with the reported DPPH-scavenging activity of AgNPs [15–16,28]. The

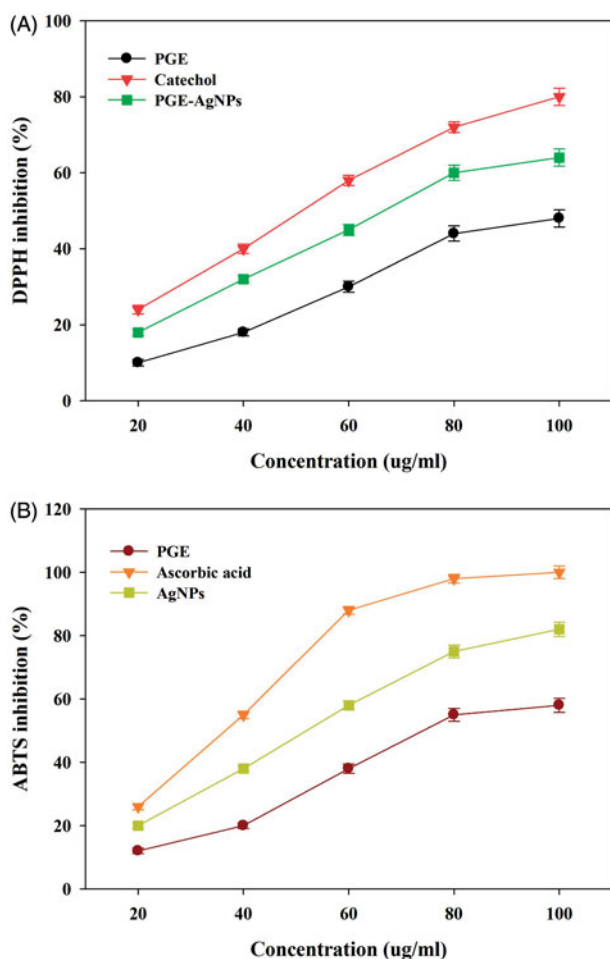


Figure 11. Antioxidant activity of synthesized PGE-AgNPs based on DPPH and ABTS radical-scavenging activities.

ABTS⁺ radicals scavenging percentage of the AgNPs found to be increased (19–81%), with an IC₅₀ value of 52 µg/mL (Figure 11(B)). The results suggest that compared to ABTS⁺, the DPPH free radical scavenging of AgNPs was more effective, with a higher IC₅₀ value. This might be due to a difference in their sensitivity towards ABTS⁺ and DPPH radicals. A considerable increase in the free radical-scavenging properties of the synthesized AgNPs against both DPPH and ABTS⁺ compared to the PGE was observed. This might suggest a combined effect of AgNPs and biomolecules present in the PGE, which increase the surface area-to-volume ratio of NPs and, in that way, interact and scavenge significantly with these free radicals. Previous studies on the radical scavenging activity of AgNPs have been reported using *Catharanthus roseus* [27], *Iresine herbstii* [14], *Clerodendrum phlomidis* [26], *Lonicera japonica* [16] and *Abutilon indicum* [15]. The above results suggest the potential application of PGE-AgNPs as alternative antioxidant compounds to develop new pharmaceutical products.

Synergistic antibacterial potential of AgNPs with standard antibiotics

The synthesized PGE-AgNPs showed significant antibacterial activity against both the Gram-negative *E. coli* (17 mm) and Gram-positive *S. aureus* (15 mm) bacteria, whereas the control (PGE) did not produce any zone of inhibition (data not shown). The difference in the zone of inhibition might be attributed to the differences in the thickness and constituents of the cell wall that exist between Gram-positive and Gram-negative bacteria and could also depend on their interaction with the charged PGE-AgNPs [9]. PGE-AgNPs with vancomycin and oxytetracycline showed a significantly enhanced zone of inhibition (40.9% and 41.5%, respectively) against both *E. coli* and *S. aureus*, respectively (Table 1). Similarly, AgNPs synthesized using *Enterococcus* sp. showed enhanced antimicrobial activity with commercial antibiotics against clinical pathogens [49]. PGE-AgNPs with streptomycin and amoxicillin showed moderate antibacterial activity against *E. coli* but were less effective against *S. aureus* (Table 1). In contrast, no enhanced effect was observed for the AgNPs with gentamicin in either bacterium (Table 1). The growth inhibition around the disc is due to the release of diffusible inhibitory compounds from AgNPs. Studies suggest that the AgNPs may interact and

Table 1. Enhanced antibacterial activity of *punica granatum* leaf extract synthesized silver nanoparticles (AgNPs) against *Escherichia coli* and *Staphylococcus aureus*.

Antibiotic (µg)	<i>E. coli</i>			<i>S. aureus</i>		
	Ab	Ab + AgNPs	Enhanced ZOI (%)	Ab	Ab + AgNPs	Enhanced ZOI (%)
Vancomycin (30)	21.0 ± 0.48 ^a	29.6 ± 0.52 ^b	40.9 ± 1.12	23.4 ± 0.48 ^a	24.8 ± 0.52 ^a	6.00 ± 0.28
Streptomycin (300)	28.2 ± 0.58 ^a	32.7 ± 0.62 ^b	15.9 ± 0.58	23.5 ± 0.52 ^a	25.4 ± 0.55 ^a	8.10 ± 0.66
Oxytetracycline (30)	32.4 ± 0.54 ^a	36.8 ± 0.48 ^b	13.5 ± 0.68	17.8 ± 0.62 ^a	25.2 ± 0.64 ^b	41.5 ± 0.88
Gentamicin (120)	28.3 ± 0.58 ^a	29.5 ± 0.52 ^a	4.20 ± 0.22	23.8 ± 0.60 ^a	23.8 ± 0.62 ^a	00
Amoxicillin + Clavulanic acid (20 + 10)	25.9 ± 0.44 ^a	30.2 ± 0.48 ^b	16.6 ± 0.45	24.8 ± 0.49 ^a	29.3 ± 0.54 ^b	18.5 ± 0.22

Ab: antibiotic; AgNPs: Silver nanoparticles; ZOI: zone of inhibition.

Values are means of three replicates ± SE.

Within a row, different letters indicate significant differences (ANOVA followed by Tukey's HSD test).

disrupt the surface of the microbial cell wall or plasma membrane, thereby inhibiting the respiration functions of the cell and disturbing DNA proteins, thereby resulting in cell death [9,35,49]. However, the exact mechanism has not been fully elucidated. Photographs of the plates loaded with selected antibiotics, as well as the AgNPs with the antibiotics, are shown in Figure S1. The above findings confirm that PGE-AgNPs are capable of rendering enhanced synergistic antibacterial activity, encouraging further explorations aimed at identifying their potential use in the preparation of antibacterial drugs.

Conclusions

Overall, AgNPs synthesized through a green route using PGE is easy, cost efficient and eco-friendly. On storage up to 4 months, synthesized AgNPs were found stable and showed no signs of aggregation, thereby increasing its potential application. The organic phytochemicals resident in the leaf extract acted and showed combined effect as a reducing and a capping agent for the AgNPs, thus avoiding any toxic chemical usage. The synthesized AgNPs showed significant antioxidant and antidiabetic activities, suggesting metal NPs as useful applications in the field of biomedical research. The green-synthesized AgNPs against the HepG2 liver cancer cell line showed remarkable cytotoxic activity *in vitro* with 50% cell mortality at 70 $\mu\text{g/mL}$. The antibacterial studies indicated that the PGE-synthesized AgNPs show potent antibacterial effect against the tested pathogens, leads to go high potential uses in biological applications. We believe that with these obtained results from the synthesized metal NPs, will lead to extend and could bring awareness toward the application of nanomaterials as alternative medicines.

Acknowledgements

This research was supported by the Agricultural Research Center funded by the Ministry of Food, Forestry, and Fisheries, Korea. The authors are thankful to Prof. Shrikrishna D. Sartale, Department of Physics, Savitribai Phule Pune University, India for availing HRTEM facility.

Disclosure statement

No potential conflict of interest was reported by the authors.

Funding

This research was supported by the Agricultural Research Center funded by the Ministry of Food, Forestry, and Fisheries, Korea, Dongguk University Research Fund of 2017 (S-2017-G0001-0001) and funded by Korea Environmental Industry & Technology Institute (A117-00197-0703-0).

References

- [1] Min Y, Caster JM, Eblan MJ, et al. Clinical translation of nanomedicine. *Chem Rev*. 2015;115:11147–11190.
- [2] Ge L, Li Q, Wang M, et al. Nanosilver particles in medical applications: synthesis, performance, and toxicity. *Int J Nanomed*. 2014;9:2399–2407.
- [3] Mirza AZ, Siddiqui FA. Nanomedicine and drug delivery: a mini review. *Int Nano Lett*. 2014;4:94.
- [4] Uchegbu IF, Schatzlein AG. Nanotechnology in drug delivery. In: Burger's medicinal chemistry, drug discovery and development. 7th ed. Hoboken: Wiley; 2010.
- [5] Guariguata L, Whiting DR, Hambleton I, et al. Global estimates of diabetes prevalence for 2013 and projections for 2035. *Diabetes Res Clin Pract*. 2014;103:137–149.
- [6] Etxeberria U, De La Garza AL, Campin J, et al. Antidiabetic effects of natural plant extracts via inhibition of carbohydrate hydrolysis enzymes with emphasis on pancreatic alpha amylase. *Expert Opin Ther Tar*. 2012;16:269–297.
- [7] Jeyaraj M, Sathishkumar GG, Sivanandhan D, et al. Biogenic silver nanoparticles for cancer treatment: an experimental report. *Colloid Surface B*. 2013;106:86–92.
- [8] Atiyeh BS, Costagliola M, Hayek SN, et al. Effect of silver on burn wound infection control and healing: review of the literature. *Burns*. 2007;33:139–148.
- [9] Kim JS, Kuk E, Yu KN, et al. Antimicrobial effects of silver nanoparticles. *Nanomedicine*. 2007;3:95–101.
- [10] Peer D, Karp JM, Hong S, et al. Nanocarriers as an emerging platform for cancer therapy. *Nat Nanotechnol*. 2007;2:751–760.
- [11] Saratale RG, Shin HS, Kumar G, et al. Exploiting fruit byproducts for eco-friendly nanosynthesis: *Citrus × clementina* peel extract mediated fabrication of silver nanoparticles with high efficacy against microbial pathogens and rat glial tumor C6 cells. *Environ Sci Pollut Res*. 2017. [Epub ahead of print]. doi: 10.1007/s11356-017-8724-z
- [12] Dauthal P, Mukhopadhyay M. Biosynthesis of palladium nanoparticles using *Delonix regia* leaf extract and its catalytic activity for nitro-aromatics hydrogenation. *Ind Eng Chem Res*. 2013;52:18131–18139.
- [13] Ajitha B, Reddy AKY, Reddy SP. Green synthesis and characterization of silver nanoparticles using *Lantana camara* leaf extract. *Mater Sci Eng C*. 2015;49:373–381.
- [14] Dipankar C, Murugan S. The green synthesis, characterization and evaluation of the biological activities of silver nanoparticles synthesized from *Iresine herbstii* leaf aqueous extracts. *Colloid Surface B*. 2012;98:112–119.
- [15] Mata R, Nakkala JR, Sadras SR. Biogenic silver nanoparticles from *Abutilon indicum*: Their antioxidant, antibacterial and cytotoxic effects *in vitro*. *Colloids Surf B Biointerfaces*. 2015;128:276–286.
- [16] Balan K, Qing W, Wang Y, et al. Antidiabetic activity of silver nanoparticles from green synthesis using *Lonicera japonica* leaf extract. *RSC Adv*. 2016;6:40162.
- [17] Atale N, Saxena S, Nirmala JG, et al. Synthesis and characterization of *Syzygium cumini* nanoparticles for its protective potential in high glucose-induced cardiac stress: a green approach. *Appl Biochem Biotechnol*. 2017;181:1140–1154.
- [18] Irvani S. Green synthesis of metal nanoparticles using plants. *Green Chem*. 2011;13:2638–2650.
- [19] Varadavenkatesan T, Selvaraj R, Vinayagam R. Phyto-synthesis of silver nanoparticles from *Mussaenda erythrophylla* leaf extract and their application in catalytic degradation of methyl orange dye. *J Mol Liq*. 2016;221:1063–1070.
- [20] Ghaedi M, Yousefinejad M, Safarpour M, et al. *Rosmarinus officinalis* leaf extract mediated green synthesis of silver nanoparticles and investigation of its antimicrobial properties. *J Ind Eng Chem*. 2015;31:167–172.
- [21] Makarov VV, Love AJ, Sinitsyna OV, et al. Green nanotechnologies: synthesis of metal nanoparticles using plants. *Acta Naturae*. 2014;6:35–44.
- [22] Saratale GD, Saratale RG, Benelli G, et al. Anti-diabetic potential of silver nanoparticles synthesized with *Argyrea nervosa* leaf extract high synergistic antibacterial activity with standard antibiotics against foodborne bacteria. *J Clust Sci*. 2017;28:1709–1727.
- [23] Edison TNJI, Lee YR, Sethuraman MG. Green synthesis of silver nanoparticles using *Terminalia cuneata* and its catalytic action in reduction of direct yellow-12 dye. *Spectrochim Acta Part A: Mol Biomol Spectro*. 2016;161:122–129.

- [24] Lopez-Miranda JL, Vazquez M, Fletes N, et al. Biosynthesis of silver nanoparticles using a *Tamarix gallica* leaf extract and their antibacterial activity. *Mater Lett.* 2016;176:285–289.
- [25] Velmurugan P, Cho M, Lim SS, et al. Phytosynthesis of silver nanoparticles by *Prunus yedoensis* leaf extract and their antimicrobial activity. *Mater Lett.* 2015;138:272–275.
- [26] Sriranjani R, Srinithya B, Vellingiri V, et al. Silver nanoparticle synthesis using *Clerodendrum phlomidis* leaf extract and preliminary investigation of its antioxidant and anticancer activities. *J Mol Liq.* 2016;220:926–930.
- [27] Al-Shmgani HSA, Mohammed WH, Sulaiman GM, Saadoon AH. Biosynthesis of silver nanoparticles from *Catharanthus roseus* leaf extract and assessing their antioxidant, antimicrobial, and wound-healing activities. *Artif Cells Nanomed Biotechnol.* 2016. [Epub ahead of print]. doi: 10.1080/21691401.2016.1220950
- [28] Saravanakumar A, Peng MM, Mani G, et al. Low-cost and eco-friendly green synthesis of silver nanoparticles using *Prunus japonica* (Rosaceae) leaf extract and their antibacterial, antioxidant properties. *Artif Cells Nanomed Biotechnol.* 2016. [Epub ahead of print]. doi: 10.1080/21691401.2016.1220950
- [29] Jurenka JS. Therapeutic applications of pomegranate (*Punica granatum* L.): a review. *Altern Med Rev.* 2008;13:28–44.
- [30] Lansky EP, Newman RA. *Punica granatum* (pomegranate) and its potential for prevention and treatment of inflammation and cancer. *J Ethnopharmacol.* 2007;109:177–206.
- [31] Das S, Barman S. Antidiabetic and antihyperlipidemic effects of ethanolic extract of leaves of *Punica granatum* in alloxan-induced non-insulin-dependent diabetes mellitus albino rats. *Indian J Pharmacol.* 2012;44:219–224.
- [32] Miller GL. Use of dinitrosalicylic acid reagent for determination of reducing sugar. *Anal Chem.* 1959;31:426–428.
- [33] Moldovan B, David L, Achim M, et al. A green approach to phyto-mediated synthesis of silver nanoparticles using *Sambucus nigra* L. fruits extract and their antioxidant activity. *J Mol Liq.* 2016;221:271–278.
- [34] Bauer AW, Kirby WMM, Sherris JC, et al. Antibiotic susceptibility testing by standardized single disc method. *Am J Clin Pathol.* 1966;45:493–496.
- [35] Otari SV, Patil RM, Ghosh SJ, et al. Green phytosynthesis of silver nanoparticles using aqueous extract of *Manilkara zapota* (L.) seeds and its inhibitory action against *Candida* species. *Mater Lett.* 2014;116:367–369.
- [36] Mittal AK, Chisti Y, Banerjee UC. Synthesis of metallic nanoparticles using plant extracts. *Biotechnol Adv.* 2013;31:346–356.
- [37] Philip D, Unni C, Aromal AS, et al. Murraya Koenigii leaf-assisted rapid green synthesis of silver and gold nanoparticles. *Spectrochim Acta A.* 2011;78:899–904.
- [38] Yang H, Ren Y, Wang T, et al. Preparation and antibacterial activities of Ag/Ag⁺/Ag³⁺ nanoparticle composites made by pomegranate (*Punica granatum*) rind extract. *Results Phy.* 2016;6:299–304.
- [39] Bar H, Bhui DK, Sahoo GP, et al. Green synthesis of silver nanoparticles using latex of *Jatropha curcas*. *Colloids Surface A.* 2009;339:134–139.
- [40] Aromal SA, Philip D. Green synthesis of gold nanoparticles using *Trigonella foenumgraecum* and its size-dependent catalytic activity. *Spectrochim Acta A.* 2012;97:1–5.
- [41] Anandalakshmi K, Venugobal J, Ramasamy V. Characterization of silver nanoparticles by green synthesis method using *Pedalium murex* leaf extract and their antibacterial activity. *Appl Nanosci.* 2016;6:399–408.
- [42] Nickavar B, Abolhasani L. Bioactivity-guided separation of an α -amylase inhibitor flavonoid from *Salvia virgata*. *Iran J Pharm Res.* 2013;12:57–61.
- [43] Rajaram K, Aiswarya DC, Sureshkumar P. Green synthesis of silver nanoparticle using *Tephrosia tinctoria* and its antidiabetic activity. *Mater Lett.* 2015;138:251–254.
- [44] Franco-Molina MA, Mendoza-Gamboa E, Sierra-Rivera CA, et al. Antitumor activity of colloidal silver on MCF-7 human breast cancer cells. *J Exp Clin Cancer Res.* 2010;29:148.
- [45] Niranjana VA, Narendhar C, Anbarasan V. Synthesis and evaluation of silver nanoparticles for the anticancer activity using *Cardiospermum halicacabum* extract. *Int J Drug Discov Herb Res.* 2012;2:504–508.
- [46] Sriram MI, ManiKanth SB, Kalishwaralal K, et al. Antitumor activity of silver nanoparticles in Dalton's lymphoma ascites tumor model. *Int J Nanomedicine.* 2010;5:753–762.
- [47] Singh H, Du J, Yi TH. Green and rapid synthesis of silver nanoparticles using *Borago officinalis* leaf extract: anticancer and antibacterial activities. *Artif Cells Nanomed Biotechnol.* 2016. [Epub ahead of print]. doi: 10.1080/21691401.2016.1228663
- [48] Dehghanizade S, Arasteh J, Mirzaie A. Green synthesis of silver nanoparticles using *Anthemis atropatana* extract: characterization and in vitro biological activities. *Artif Cells Nanomed Biotechnol.* 2017;1–9.
- [49] Rajeshkumar S, Malarkodi C, Vanaja M, et al. Anticancer and enhanced antimicrobial activity of biosynthesized silver nanoparticles against clinical pathogens. *J Mol Struct.* 2016;1116:165–173.